The ARM Data-oriented Metrics and Diagnostics Package for Climate Models

- A New Tool for Evaluating Climate Models with Field Data

C. Zhang, S. Xie, C. Tao, S. Tang, T. Emmenegger, J. D. Neelin, K. A. Schiro, W. Lin and Z.

Shaheen

Affiliations:

Zhang, Xie, Tao, Tang, Shaheen – Lawrence Livermore National Laboratory, Livermore,

California;

Emmenegger, Neelin – University of California, Los Angeles, California;

Schiro – Jet Propulsion Laboratory, California Institute of Technology, Pasadena, California;

Lin – Brookhaven National Laboratory, Upton, New York;

*Now at Google LLC.

Corresponding author: *Chengzhu Zhang, Atmospheric, Earth and Energy Division (L-103),*

Lawrence Livermore National Laboratory, Livermore, CA 94550.

E-mail: zhang40@llnl.gov

27 **ABSTRACT.** The U.S. Department of Energy (DOE) Atmospheric Radiation Measurement

28 (ARM) program produces ground-based long-term contiguous unique measurements for

29 atmospheric state, precipitation, turbulent fluxes, radiation, aerosol, cloud and the land surface,

30 which are collected at its multiple Climate Research Facilities. These comprehensive datasets have

31 been widely used to calibrate climate models and are proven to be invaluable for climate model

32 development and improvement. This article introduces an evaluation package to facilitate the use

33 of ground-based ARM measurements in climate model evaluation.

34

35 The ARM data-oriented metrics and diagnostics package (ARM-DIAGS) includes both ARM

36 observational datasets and a Python-based analysis toolkit for computation and visualization. The

37 observational datasets are compiled from multiple ARM data products and specifically tailored for

38 use in climate model evaluation. In addition, ARM-DIAGS also includes simulation data from

39 models participating the Coupled Model Inter-comparison Project (CMIP), which will allow

40 climate-modeling groups to compare a new, candidate version of their model to existing CMIP

41 models. The analysis toolkit is designed to make the metrics and diagnostics quickly available to

42 the model developers.

43

1. Introduction

A set of standard metrics and diagnostics provides an effective way for climate modeling centers to routinely assess their model performance and judge the improvement of model simulations from new parameterizations. In the past, climate model developers have often relied on satellite remote sensing products to calibrate and tune their models. Satellite data sets provide a great global coverage, however, it is difficult to apply satellite data in some process studies due to their poor temporal resolutions. Therefore, utilizing detailed high-frequency ground-based measurements for a comprehensive collection of quantities can be a complementary test in model evaluation.

Over the past three decades, the U.S. Department of Energy (DOE) Atmospheric Radiation Measurement (ARM) program has established several permanent research sites and deployed a number of ARM Mobile Facilities (AMF) in diverse climate regimes around the world to collect long-term continuous field measurements of clouds, aerosols, and radiation and their associated large-scale environments. These detailed field observations have provided a unique observational basis specifically for understanding cloud and precipitation related processes and evaluating and improving their representations in climate models. However, ARM data have not been extensively utilized in current model development workflows. With the growing interest in the climate modeling community in developing process-oriented metrics and diagnostics to aid parameterization developments (Maloney et al. 2019), the high-frequency process-oriented ARM observations should play a more important role in the future metrics and diagnostics development.

In this article, we introduce the recently developed ARM data-oriented metrics and diagnostics package (ARM-DIAGS) for the global climate community to facilitate the use of ARM field data in climate model evaluation. The focus is on ARM unique observations on clouds and aerosols, as

67 well as process-oriented diagnostics that are particularly aimed to improve the representation of

68 cloud and precipitation related processes in climate models, such as those included in the Coupled

69 Model Inter-comparison Project (CMIP). The package is available publicly with the hope that it

70 can serve as an easy entry point for climate modelers to compare their models with ARM data and

71 supplemented CMIP datasets.

72

73 **2. Overview of the ARM data-oriented metrics and diagnostics package**

74 The ARM-DIAGS development closely follows the CMIP protocol to efficiently distribute

75 ARM metrics and diagnostics package along with other metrics packages to the CMIP community

76 and other climate modeling centers. For this purpose, the diagnostic toolkit is built with the Python

77 programming language and utilizes Python libraries for scientific analysis (such as NumPy and

78 matplotlib). Additional Python packages developed by DOE (i.e., the Community Data Analysis

79 Tools (CDAT), https://cdat.llnl.gov/) are also used. Four components are currently included in the

80 ARM-DIAGS: 1) a Python-based analysis program; 2) an ARM-based collection of mean and

81 diurnal and seasonal cycle climatologies as well as high time frequency data for process-oriented

82 diagnostics; 3) a database of simulation data from models contributed to CMIP project; and 4)

83 relevant technical documentations for ARM-DIAGS.

84 The observations used to assess model performance primarily rely on the ARM Best Estimate

85 (ARMBE) data products (Xie et al. 2010) and other ARM value-added products (VAPs)

86 (https://www.arm.gov/capabilities/vaps), which are available for all the ARM permanent research

87 sites and some ARM mobile facilities. These data often rely on measurements at the ARM Central

88 Facility (CF) locations (i.e., single point measurements). To improve model-observation

89 comparison, the ARM long-term continuous forcing data (Xie et al. 2004), which represents an

90   average over a Global Climate Model (GCM) grid box, is also used when it is available. For cloud

91   properties such as cloud liquid and ice water contents, the ARM Cloud Retrieval Ensemble Data

92   (ACRED) (Zhao et al. 2012) is used. The detailed information about ARM data used in the ARM-

93   DIAGS package is listed in Tables 1a and 1b. The observational data product consists of hourly

94   averaged, diurnal cycle, monthly means or climatological summaries of the measured quantities,

95   with variable names, units and vertical dimensions remapped to CMIP convention. They are

96   currently available for the Southern Great Plains (SGP) site (Table 1a) as well as the North Slope

97   of Alaska (NSA) Barrow site and the Tropical Western Pacific (TWP) Manus, Nauru, and Darwin

98   sites (Table 1b). Other than the ARM observations, ARM-DIAGS also includes simulation data

99   from models participating CMIP project, which will allow climate-modeling groups to compare a

100   new candidate version of their model to existing CMIP models. A full list of metrics and

101   diagnostics are as follows, with a subset demonstrated in Section 3 of this article.

102   - A set of basic metrics tables: mean, mean bias, correlation and root mean square error

103   based on annual cycle of each variable.

104   - Line plots and Taylor Diagrams (Taylor, 2001) for annual cycle variability of each

105   variable.

106   - Contour and vertical profiles of annual cycle and diurnal cycle of cloud fraction.

107   - Line and harmonic dial plots (Covey et al. 2016) of diurnal cycle of precipitation.

108   - Probability Density Function plots of precipitation rate (Pendergrass et al. 2014)

109   - Convection onset metrics showing statistical relationship between precipitation rate

110   and column water vapor (Schiro et al. 2016)

111

112   **3. Facilitating use of ARM data in climate model evaluation**

113 *Diagnosis of summertime warm bias*. The data and diagnostics provided through ARM-DIAGS

114 have been used for studying the systematic warm bias in surface temperature found among the

115 climate models in summertime at mid-latitude continent including the ARM SGP site (Zhang et

116 al. 2018). The biases are consistent with both overestimated surface shortwave radiation and

117 underestimated evaporative fraction, which contribute to the warm bias as illustrated in Figure 1.

118 These diagnostics provide an integrated picture with detailed field observations to identify possible

119 model deficiency in representing cloud, radiation, and land properties, as well as their interactions.

120

121 *Diurnal cycle of cloud fraction*: This daily cycle could serve as a critical test of the models'

122 representation of the physical processes controlling cloud life cycle. One unique product from

123 ARM is cloud vertical profile measurements derived from an integration of multiple active remote

124 sensors, including Millimeter wavelength cloud radars, laser ceilometers and Micropulse Lidars

125 (Active Remote Sensing of Clouds product, ARSCL). Figure 2 shows a comparison between

126 observed and simulated diurnal cycle of cloud vertical structure over the ARM midlatitude and

127 tropical sites (i.e., SGP and Manus), where prominent climatological diurnal cycle of clouds is

128 present. Over the SGP site, a lack of shallow to deep cloud transition during summertime (June-

129 July-August) is shown in E3SM. This is a common model bias which is related to model deep

130 convection that is triggered too easily and does not allow low clouds to build-up. The Manus site

131 exhibits a strong diurnal cycle, with a maximum in low cloud fraction occurring at early local noon

132 and followed by a maximum in high cloud hours later. Similarly, the model in general

133 underestimated the lower cloud and overestimated high cloud, which is also lack of diurnal

134 variability.

135 *Diurnal cycle of precipitation*. Diurnal cycle of precipitation is often served as a benchmark for

136 climate models. The diurnal cycle diagnostics in ARM-DIAGS, which compare the precipitation

137 intensity and its peak time, have been utilized by the Energy Exascale Earth System Model (E3SM)

138 development team to assess the performance of a newly developed convection triggering

139 mechanism (Xie et al. 2019). Figure 3 shows that all climate models including the default E3SM

140 are not able to capture the observed nocturnal peak which is often associated with the eastward

141 propagation of mesoscale convective systems. A recently developed convective triggering

142 function, which incorporates an empirical dynamic constraint and allows elevated convection to

143 be captured, started to pick up the early morning peak time, although the intensity is still too weak.

144 These diagnostics are useful to repeat continually, especially when new features in convection

145 parameterizations are implemented.

146

147 *Precipitation distribution*. The probability density function analysis for daily mean precipitation

148 at the SGP site during June-July-August is shown in Figure 4. This example illustrates that models

149 tend to underestimate heavy rainfall (>10 mm per day) occurrences which contribute more to the

150 total precipitation amount than lighter rainfall occurrence. The overlaying result from GPCP

151 (Global Precipitation Climatology Project One-Degree Daily Precipitation Data Set) also confirms

152 this systematic model bias.

153
154 *Convection onset metrics.* Convection onset metrics allow users to compare diagnostics for the

155 behavior of deep convection from ARM observations to model output. The statistics quantify

156 robust relationships between precipitation, column water vapor (CWV) and temperature. This

157 includes the sharp increase or "pickup" in conditional-average precipitation rate above a critical

158 CWV value seen in Figure 5a, which is easily identifiable for short time averages at tropical ARM

159 sites. The pickup represents the onset of conditional instability yielding strong convective

160 precipitation (Schiro et al. 2016) and is also seen in the probability of precipitation (Figure 5b).

161 The probability density of CWV and the contribution from precipitating points (Figure 5c) have a

162 drop in probability density at high CWV corresponding to the regime with high precipitation loss

163 above critical.

164 The statistics discussed here can distinguish between models' convective parametrizations and

165 their qualitative characteristics are robust to space and time averaging (Kuo et al. 2018). An

166 example of model comparison is given in Figure 5. An important diagnostic in the model

167 evaluation of convection onset concerns the critical CWV value where the precipitation pickup

168 begins. Many models exhibit a pickup at lower CWV than observations (Kuo et al. 2020), as seen

169 in Figure 5a for E3SM. This mismatch persists even when temperature dependence (not shown but

170 will be included in a feature release of ARM-DIAGS) is included by binning by the saturation

171 water vapor.

172
173 **4. Summary and future work**

174 The ARM metrics and diagnostics package is designed and developed to facilitate the use of ARM

175 ground-based in-situ measurements in climate model evaluation. Metrics and diagnostics

176 evaluating the simulated atmospheric and cloud fields are generated by running a Python program

177 in a simple software environment based on CDAT. The v2.0 ARM-DIAGS's analysis codes are

178 currently publicly available through GitHub (https://github.com/ARM-DOE/arm-gcm-

179 diagnostics) under the ARM User Facility project space. Analysis data include ARM observational

180 datasets and the reference CMIP5 AMIP data can be downloaded through the ARM archive

181 (https://www.arm.gov/capabilities/vaps/adcme-123). For now, the default requirement for the

182 input model is that the data are under CMIP conventions. Anyone interested in applying ARM-

183 DIAGS to a specific model should contact the development team via our GitHub page for specific

184 configurations for a model run.

185 Future work includes extending the ARM-DIAGS to the ARM Eastern North Atlantic (ENA) site

186 (a new fixed site) and ARM AMF sites. CMIP6 data will be included as it becomes available. The

187 diagnostics suite will be continuously improved with close collaboration with scientists in the field.

188 Ongoing work includes incorporation of the recently developed ARM cloud radar simulator (Y.

189 Zhang et al. 2018) into ARM-DIAGS to improve the comparison between model clouds and ARM

190 cloud radar observations, as well as adding temperature dependence to convection onset statistics.

191 In addition, utilizing other sources of observations, such as those retrieved from satellites, as

192 supplementary data, can help address issues associated with observation uncertainty and data

193 resolution.

194

For Further Reading:

Bond, D. (2005), Soil Water and Temperature System (SWATS) Handbook, ARM Technical Report TR-063, U.S. Department of Energy,Washington, D. C.

Cook, D. R. (2011a). Energy Balance Bowen Ratio Station (EBBR) Handbook (No. DOE/SC-ARM/TR-037). DOE Office of Science Atmospheric Radiation Measurement (ARM) Program (United States).

Cook, D. R. (2011b). Eddy Correlation Flux Measurement System (ECOR) Handbook (No. DOE/SC-ARM/TR-052). DOE Office of Science Atmospheric Radiation Measurement (ARM) Program (United States).

Covey, C., Gleckler, P. J., Doutriaux, C., Williams, D. N., Dai, A., Fasullo, J., ... & Berg, A. (2016). Metrics for the diurnal cycle of precipitation: Toward routine benchmarks for climate models. *Journal of Climate*, *29*(12), 4461-4471.

Clothiaux, E. E., T. P. Ackerman, G. G. Mace, K. P. Mo- ran, R. T. Marchand, M. Miller, and B. E. Martner, 2000: Objective determination of cloud heights and radar reflectivities using a combination of active remote sensors at the ARM CART sites. J. Appl. Meteor., 39, 645–665.

Chandra, A. S., C. Zhang, S. A. Klein, and H.-Y. Ma (2015), Low-cloud characteristics over the tropical western Pacific from ARM observations and CAM5 simulations, J. Geophys. Res. Atmos., 120, 8953–8970, doi:10.1002/2015JD023369.

Knootz, et al. (2013), Aerosol Optical Depth Value-Added Product, DOE/SC-ARM/TR-129, USDOE Office of Science, Washington, D. C.

Kuo, Y. H., Schiro, K. A., & Neelin, J. D. (2018). Convective transition statistics over tropical oceans for climate model diagnostics: Observational baseline. *J. Atmos. Sci.*, *75*, 1553-1570.

Kuo, Y. H., Neelin, J. D., Chen, C. C., Chen, W.T , Donner, L. J. , Gettelman, A , Jiang, X , Kuo, K. T., Maloney, E. , Mechoso, C. R. , Ming, Y., Schiro, K. A., Seman, C. J. , Wu, C. M., & Zhao, M. (2020). Convective transition statistics over tropical oceans for climate model 2 diagnostics: GCM evaluation, *J. Atmos. Sci.*, *77*, 379-403.

Long, C. N. and Y. Shi, (2006): The QCRad Value Added Product: Surface Radiation Measurement Quality Control Testing, Including Climatologically Configurable Limits, Atmospheric Radiation Measurement Program Technical Report, ARM TR-074, 69 pp.

Long, C. N., and Y. Shi, (2008): An Automated Quality Assessment and Control Algorithm for Surface Radiation Measurements, TOASJ, 2, 23-37, doi: 10.2174/1874282300802010023.

246 Maloney, E. D., Gettelman, A., Ming, Y., Neelin, J. D., Barrie, D., Mariotti, A., ... & Annamalai,
247 H. (2019). Process-Oriented Evaluation of Climate and Weather Forecasting Models. *Bulletin of*
248 *the American Meteorological Society*, *100*(9), 1665-1686.
249
250 Pendergrass, A. G., & Hartmann, D. L. (2014). Two modes of change of the distribution of rain.
251 Journal of Climate, 27(22), 8357-8371.
252
253 Schiro, K. A., Neelin, J. D., Adams, D. K., & Lintner, B. R. (2016). Deep convection and column
254 water vapor over tropical land versus tropical ocean: A comparison between the Amazon and the
255 tropical western Pacific. Journal of the Atmospheric Sciences, 73(10), 4043-4063.
256
257 Taylor, K. E. (2001), Summarizing multiple aspects of model performance in a single diagram,
258 J. Geophys. Res., 106(D7), 7183– 7192, doi:10.1029/2000JD900719.
259
260
261 Xie, S., Wang, Y. C., Lin, W., Ma, H. Y., Tang, Q., Tang, S., ... & Zhang, M. (2019). Improved
262 Diurnal Cycle of Precipitation in E3SM with a Revised Convective Triggering Function. Journal
263 of Advances in Modeling Earth Systems.
264
265 Xie, S., McCoy, R. B., Klein, S. A., Cederwall, R. T., Wiscombe, W. J., Jensen, M. P., ... &
266 Mather, J. H. (2010). Clouds and more: ARM climate modeling best estimate data: A new data
267 product for climate studies. Bulletin of the American Meteorological Society, 91(1), 13-20.
268
269 Xie, S. C., R. T. Cederwall, and M. H. Zhang (2004), Developing long-term single-column
270 model/cloud system-resolving model forcing data using numerical weather prediction products
271 constrained by surface and top of the atmosphere observations, Journal of Geophysical Research-
272 Atmospheres, 109(D1), doi: 10.1029/2003jd004045.
273
274 Zhang, C., and Xie, S., (2017). ARM Data-Oriented Metrics and Diagnostics Package for Climate
275 Model Evaluation Value-Added Product. Ed. by Robert Stafford, ARM Climate Research Facility.
276 DOE/SC-ARM-TR-202.
277
278 Zhang, C., Xie, S., Klein, S. A., Ma, H. Y., Tang, S., Van Weverberg, K., ... & Petch, J. (2018).
279 CAUSES: diagnosis of the summertime warm bias in CMIP5 climate models at the ARM southern
280 great plains site. Journal of Geophysical Research: Atmospheres, 123(6), 2968-2992.
281
282 Zhang, Y., Xie, S., Klein, S. A., Marchand, R., Kollias, P., Clothiaux, E. E., ... & Tang, S. (2018).
283 The ARM Cloud Radar Simulator for Global Climate Models: Bridging Field Data and Climate
284 Models. *Bulletin of the American Meteorological Society*, *99*(1), 21-26.
285
286 Zhao, C., Xie, S., Klein, S. A., Protat, A., Shupe, M. D., McFarlane, S. A., ... & Hogan, R. J.
287 (2012). Toward understanding of differences in current cloud retrievals of ARM ground- based
288 measurements. *Journal of Geophysical Research: Atmospheres*, *117*(D10).
289
290
291

Figure Captions Lists:

Figure 1: Annual cycle of monthly mean of (a) surface air temperature, (b) precipitation, (c) surface air relative humidity, (d) surface downward shortwave radiative flux, (e) surface sensible flux, and (f) surface latent heat flux over the ARM SGP domain (averaged over 35-38°N, 99-96°W) from ARM observation averaged over 1999 to 2011 (red line with error bars representing one standard deviation of inter-annual variability) and CMIP5 simulations averaged over 1979 to 2008 (grey lines for individual CMIP5 models and black line for multi-model mean). JJA mean values are shown in the legend. Plots are modified from Zhang et al. (2018).

Figure 2: Climatological composite diurnal cycle of clouds from observed (left panel) and simulated by E3SM (right panel). JJA mean at SGP (row 1); Annual mean at Manus (row 2).

Figure 3: Left: black dots are ARM observation. Curves are the first harmonics: grey for CMIP5 model AMIP type of runs. Color curves are from DOE's E3SM Atmosphere Model (EAM v1) with a standard control run and a run using newly developed convection triggers (Detailed experiment description can be found in (Xie et. al., 2019). Right: mapping precipitation peak time and amplitude from the first harmonics to polar coordinate.

Figure 4: Daily-Mean precipitation frequency (a) and precipitation amount (b) as a function of precipitation rate using observations from ARM (blue line) and GPCP (red line) compared with CMIP5 AMIP simulations shown as gray lines. The black line represents the multi-model mean. The precipitation bin arrangement follows method described by Pendergrass et al. (2014).

313   Figure 5: (a) Precipitation conditionally averaged on column water vapor (CWV) for observations

314   indicated by color-coded dots (ARMBE precipitation and gap filled MWRRET radiometer CWV)

315   and E3SM model output (black) over Manus Island. (b) as in (a) but for precipitation probability.

316   (c) The PDFs of CWV for observations (dark blue) and model (black) and of the contribution to

317   this from points with precipitation exceeding 0.5 mm/hr for observations (light blue) and model
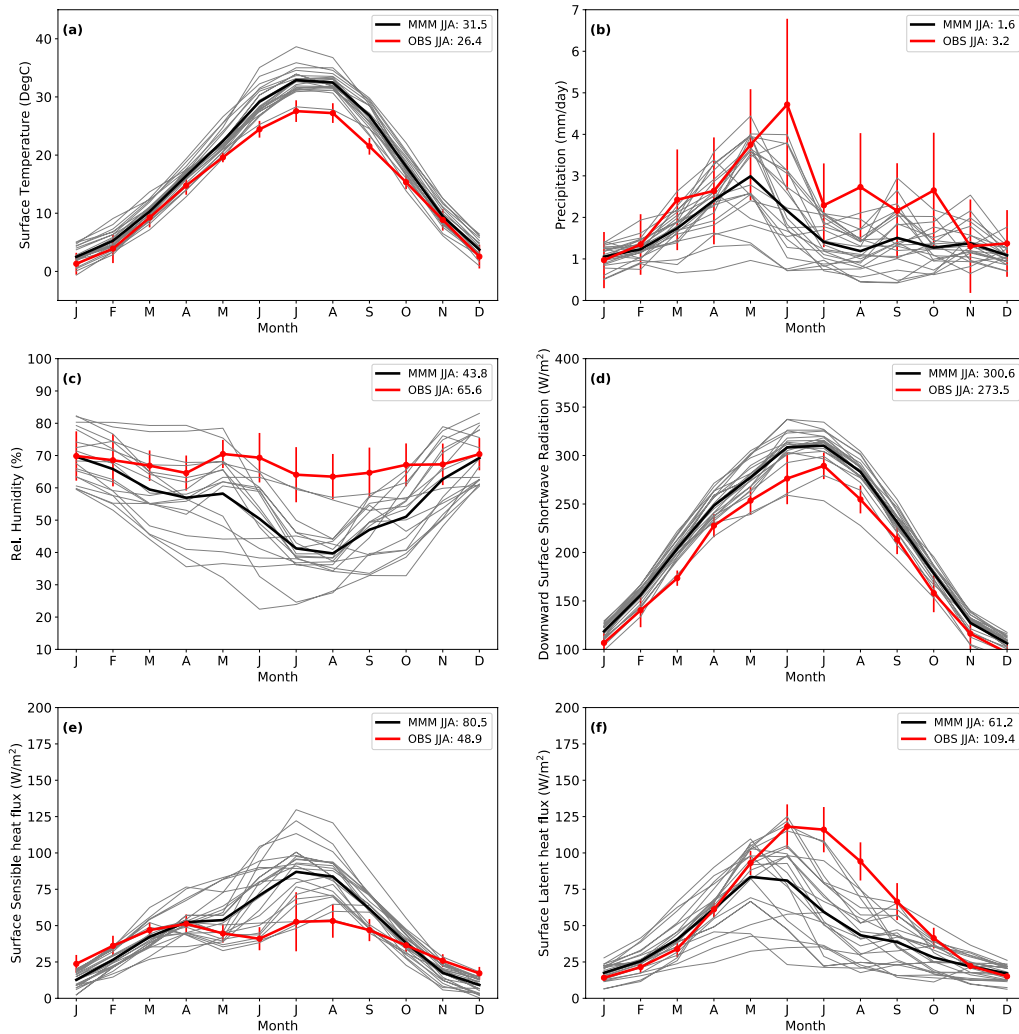
318   (grey).

319

320
321 Figure 1: Annual cycle of monthly mean of (a) surface air temperature, (b) precipitation, (c) surface

322 air relative humidity, (d) surface downward shortwave radiative flux, (e) surface sensible flux, and

323 (f) surface latent heat flux over the ARM SGP domain (averaged over 35-38°N, 99-96°W) from

324 ARM observation averaged over 1999 to 2011 (red line with error bars representing one standard

325 deviation of inter-annual variability) and CMIP5 simulations averaged over 1979 to 2008 (grey

326 lines for individual CMIP5 models and black line for multi-model mean). JJA mean values are

327 shown in the legend. Plots are modified from Zhang et al. (2018).
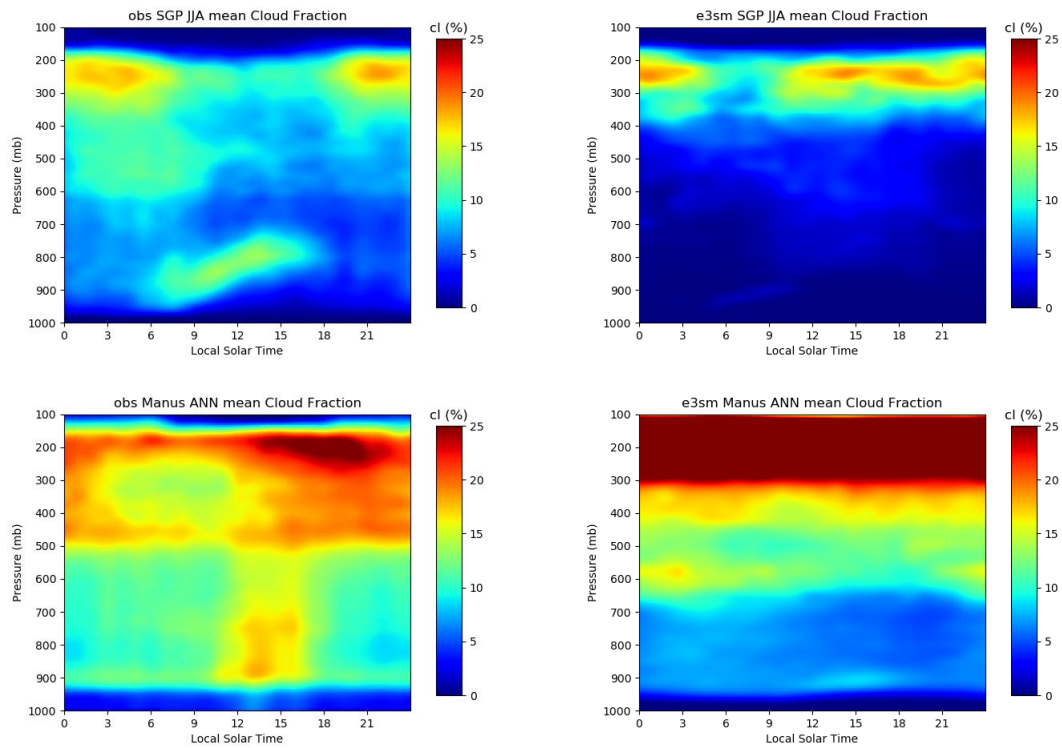
328

14

Figure 2: Climatological composite diurnal cycle of clouds from observed (left panel) and simulated by E3SM (right panel). JJA mean at SGP (row 1); Annual mean at Manus (row 2).
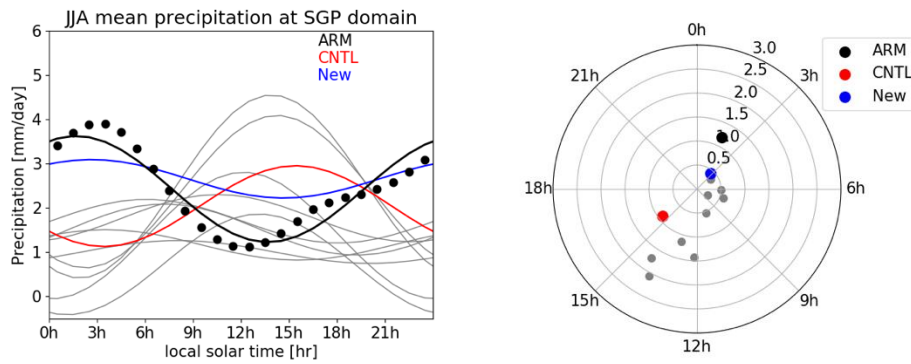
332

Figure 3: Left: black dots are ARM observation. Curves are the first harmonics: grey for CMIP5

model AMIP type of runs. Color curves are from DOE's E3SM Atmosphere Model (EAM v1)

with a standard control run and a run using newly developed convection triggers (Detailed

experiment description can be found in (Xie et. al., 2019). Right: mapping precipitation peak

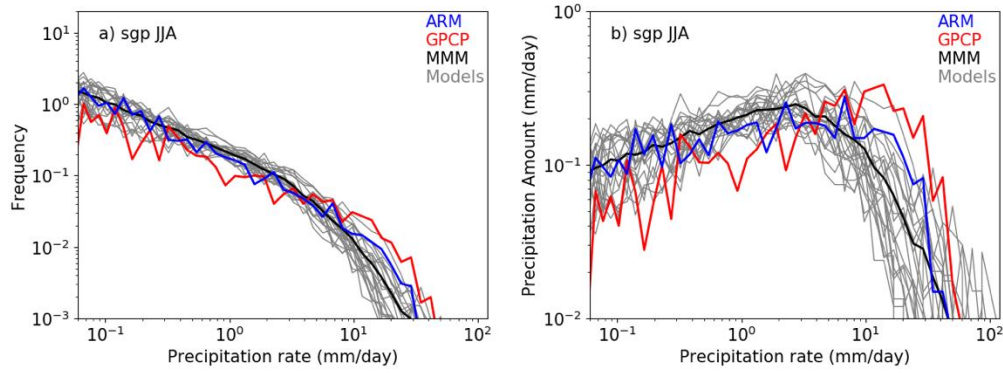time and amplitude from the first harmonics to polar coordinate.

341

342 Figure 4: Daily-Mean precipitation frequency (a) and precipitation amount (b) as a function of

343 precipitation rate using observations from ARM (blue line) and GPCP (red line) compared with

344 CMIP5 AMIP simulations shown as gray lines. The black line represents the multi-model mean.

345 The precipitation bin arrangement follows method described by Pendergrass et al. (2014).
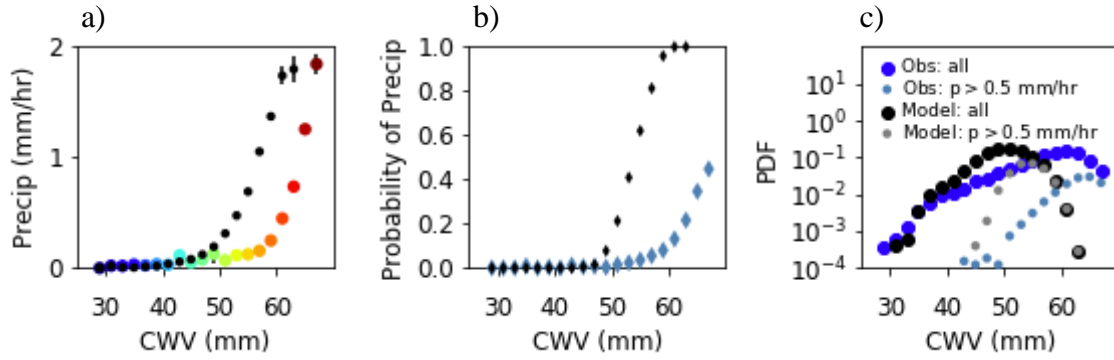
346

347

348 Figure 5: (a) Precipitation conditionally averaged on column water vapor (CWV) for observations

349 indicated by color-coded dots (ARMBE precipitation and gap filled MWRRET radiometer CWV)

350 and E3SM model output (black) over Manus Island. (b) as in (a) but for precipitation probability.

351 (c) The PDFs of CWV for observations (dark blue) and model (black) and of the contribution to

352 this from points with precipitation exceeding 0.5 mm/hr for observations (light blue) and model

353 (grey).

354

355   Table 1a

Quantities	M Data Products	Data Source/ Instruments	Time resolution	Spatial info
Surface Screen-Level Temperature/ Humidity	ARM Continuous forcing dataset	Surface Meteorological Observation System (SMOS), Oklahoma and Kansas mesonet stations (OKM and KAM)[Xie et al. 2004]	mon, day, hr	sgp domain averaged
Temperature/Humidity profile/wind speed/large scale tendencies	Same as above	NOAA/ NCEP Rapid Update Cycle (RUC) analysis data [Xie et al. 2004]	mon, day, hr	sgp domain averaged
Surface Precipitation	Same as above	Arkansas-Red Basin River Forecast Center (ABRFC) Nexrad radar precipitation estimates w/ rain gauge	mon, day, hr	sgp domain averaged
Precipitable Water	Same as above	Microwave Radiometer (MWR) water liquid & vapor along line of sight (LOS) path (MWRLOS)	mon, day, hr	sgp domain averaged
Surface All Sky Radiative Fluxes	Same as above	Data Quality Assessment for ARM Radiation Data (QCRAD) [Long and Shi, 2006, 2008]	mon, day, hr	sgp domain averaged
Aerosol Optical Depth 550nm	MFRSRAOD1M ICH	Multifilter Rotating Shadowband Radiometer (MFRSR) [Knootz et al.,2013]	mon	Averaged over sgp Site C1 and E13
Surface Latent/Sensible Heat	BAEBBR	Best-Estimate Fluxes From EBBR Measurements and Bulk Aerodynamics Calculations (BAEBBR) [Cook, 2011a]	mon	sgp domain averaged
	QCECOR	Quality Controlled Eddy Correlation Flux Measurement [Cook, 2011b]	mon	sgp domain averaged
Surface Soil Moisture Content (10 cm)	SWATS	Soil Water and Temperature System (SWATS)) [Bond, 2005]	mon	sgp domain averaged
Cloud Fraction	ARSCL	Active Remote Sensing of Clouds [Clothiaux et al, 2001]	mon, day, hr	sgp Site C1
Ice Water Content/Liquid Water Content	ACRED	ARM Cloud Retrieval Ensemble Dataset [Zhao et al. 2012]	mon, day, hr	sgp Site C1

356
357

358

359   Table 1b

Quantities	ARM Data Products	Data Source/ Instruments	Time resolution	Spatial info
Surface Screen-Level Temperature/ Humidity	ARMBE-ATM	ARM-standard meteorological instrumentation at the surface [Xie et al. 2010]	mon	twp C1; nsa C1
Surface Precipitation	ARMBE-ATM	Same as above	mon, hr	twp C1; nsa C1
Precipitable Water	ARMBE-ATM	Microwave Radiometers Retrievals (MWRRET) [Xie et al. 2010]	mon, hr	twp C1; nsa C1
Surface Radiative Fluxes	ARMBE-CLD	Data Quality Assessment for ARM Radiation Data (QCRAD) [Long and Shi, 2006, 2008]	mon	twp C1; nsa C1
Cloud Fraction	ARSCL	Active Remote Sensing of Clouds [Clothiaux et al, 2001]	mon, hr	twp C1; nsa C1

360

361   Table 1: Observed quantities selected in the evaluation package, including the quantity names,

362   the data sources, and the temporal and spatial information of the data. (a) for SGP and (b) for

363   NSA and TWP sites.